

Polarization-sensitive photophoresis

Vladlen G. Shvedov, Cyril Hnatovsky, Niko Eckerskorn, Andrei V. Rode, and Wieslaw Krolikowski

Citation: *Applied Physics Letters* **101**, 051106 (2012); doi: 10.1063/1.4742137

View online: <http://dx.doi.org/10.1063/1.4742137>

View Table of Contents: <http://scitation.aip.org/content/aip/journal/apl/101/5?ver=pdfcov>

Published by the [AIP Publishing](#)

Articles you may be interested in

[Trapping of individual airborne absorbing particles using a counterflow nozzle and photophoretic trap for continuous sampling and analysis](#)

Appl. Phys. Lett. **104**, 113507 (2014); 10.1063/1.4869105

[Photophoretic trampoline—Interaction of single airborne absorbing droplets with light](#)

Appl. Phys. Lett. **101**, 131115 (2012); 10.1063/1.4755761

[Polarization-sensitive photoresponse of nanographite](#)

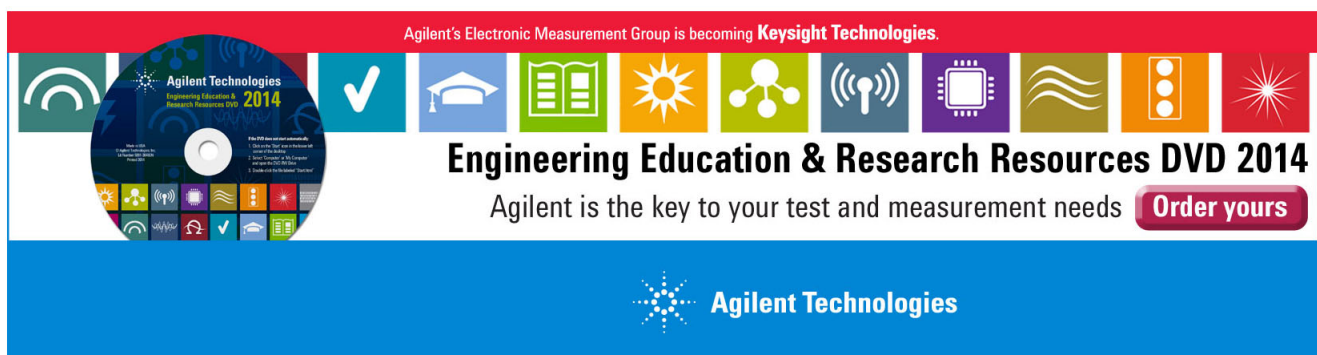
Appl. Phys. Lett. **98**, 091903 (2011); 10.1063/1.3559928

[Selective optical trapping based on strong plasmonic coupling between gold nanorods and slab](#)

Appl. Phys. Lett. **98**, 083117 (2011); 10.1063/1.3559602

[Electrophoretic mobility of a growing cell studied by photonic force microscope](#)

Appl. Phys. Lett. **97**, 203704 (2010); 10.1063/1.3519474

The advertisement features a red header with the text 'Agilent's Electronic Measurement Group is becoming Keysight Technologies.' Below this is a row of icons representing various engineering and research fields: a green Wi-Fi symbol, a blue checkmark, a blue graduation cap, a green book, a yellow sun, a green network diagram, a blue antenna, a purple microchip, a green wave, an orange vertical bar, and a red starburst. To the left of these icons is a DVD image with the text 'Agilent Technologies Engineering Education & Research Resources DVD 2014'. Below the icons, the text reads 'Engineering Education & Research Resources DVD 2014' and 'Agilent is the key to your test and measurement needs' with an 'Order yours' button. The bottom of the advertisement is a blue banner with the Agilent Technologies logo and name.

Polarization-sensitive photophoresis

Vladlen G. Shvedov, Cyril Hnatovsky,^{a)} Niko Eckerskorn, Andrei V. Rode, and Wieslaw Krolikowski

Laser Physics Centre, Australian National University, Canberra ACT 0200, Australia

(Received 17 June 2012; accepted 17 July 2012; published online 31 July 2012)

We photophoretically trap spherical airborne particles using a single radially or azimuthally polarized laser beam and show that the trapping efficiency is significantly higher for the radial polarization. The demonstrated polarization sensitivity of the photophoretic force, which is caused by polarization-dependent reflection from the particles, adds additional flexibility to the optical micromanipulation of light absorbing particles in gaseous media. © 2012 American Institute of Physics. [<http://dx.doi.org/10.1063/1.4742137>]

Optical manipulation of light absorbing particles in gaseous media is dominated by the photophoretic force,^{1,2} which results from uneven heating of the illuminated particles in the light field. This force is typically orders of magnitude larger than the force associated with light pressure.^{1,2} When the particle size is much greater than the mean free path of the surrounding gas molecules (i.e., low Knudsen number), a temperature gradient in the gas, created by the particle, causes the gas to flow along the particle surface.³ The hydrodynamics of this gas motion determines the magnitude of the photophoretic force.

Despite the well known ability of the photophoretic force to affect the motion of or levitate relatively large (10 μm) and heavy (10 ng) absorbing particles in gases at a light intensity as low as $\sim 1 \text{ W/cm}^2$,² studies on its use for optical tweezing have been sparse until recently. In fact, Ashkin in his seminal article on acceleration and trapping of particles by radiation pressure deliberately worked with transparent objects to minimize the effect of photophoresis.¹ Such a prolonged neglect of the photophoretic force can be explained by the fact that for strongly absorbing particles, it is repulsive (i.e., positive photophoresis) and tends to push them away from the regions of maximum light intensity, thus precluding optical trapping and manipulation with beams having a Gaussian intensity profile. The problem was solved using light fields with complex intensity distributions, which allow absorbing particles to be pulled into and then trapped inside intensity minima.^{2,4-8} The trapped particles can then be moved either together with the light field as a whole or by changing the light field itself.^{7,8}

The dependence of the photophoretic force on the characteristics of both the acted-upon particle, the surrounding gas and the light field has been a subject of extensive studies.⁹⁻¹³ As far as the light field is concerned, only two of its major parameters, namely, the wavelength and the intensity distribution, have been discussed in the above context so far.¹¹⁻¹³

In this letter, we show that the photophoretic force is strongly affected by the polarization state of the driving light field. We demonstrate this effect by measuring changes in the efficiency of a photophoretic trap based on a cylindrical

vector beam whose state of polarization can be varied while keeping the intensity and other parameters unchanged. This work extends and generalizes our previous experiments on transport of spherical particles in air with two counter-propagating optical vortex beams having orthogonal linear polarizations.¹⁴

The experiments which follow have been carried out in ambient air with large hollow glass spheres 80–110 μm in diameter coated with carbon. In this very low Knudsen number regime, the photophoretic force on a spherical particle exposed to one-sided electromagnetic radiation can be approximated by^{3,13,15}

$$F = 9\mu_a^2 P_{abs}/4a\rho_a T (k_p + 2k_a), \quad (1)$$

where P_{abs} is the total power absorbed by the particle, a and k_p are the particle radius and thermal conductivity, μ_a and ρ_a denote, respectively, the gas (i.e., air) viscosity and density, and T stands for the average gas temperature near the particle surface.

We performed our experiments in the optical levitation geometry shown in Fig. 1(a). To levitate particles, we used either a radially or azimuthally polarized continuous wave 532-nm laser beam with a doughnut intensity profile given by¹⁶

$$I(r, z) = P \left(r^2/\pi w^4(z) \right) \exp \left(-r^2/w^2(z) \right). \quad (2)$$

In expression (2), P is the total power in the beam, $w(z) = w_0(1 + z^2\lambda^2/(4\pi^2 w_0^4))^{1/2}$ is the radius of the maximum intensity contour at a distance z -from the beam waist, w_0 denotes $w(0)$, λ is the wavelength of light, and r is the radial distance from the center axis of the beam. A detailed description of the method which allows one to synthesize radially or azimuthally polarized beams by means of a uniaxial crystal can be found elsewhere.¹⁶ Importantly, just by rotating the second half-wave plate after the pinhole (see Fig. 1(a)), one can change the polarization state of the beam, for instance, from azimuthal to radial without affecting its intensity profile whatsoever,¹⁷ as demonstrated in Fig. 1(b). Figure 1(c) shows that the expression for $w(z)$ accurately describes how the radius of the generated beam changes with z and, therefore, validates its use for the calculations that we present below.

^{a)}Author to whom correspondence should be addressed. Electronic mail: chn111@physics.anu.edu.au.

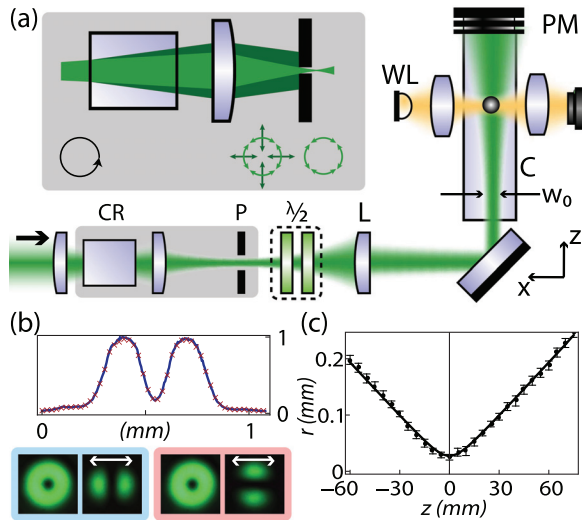


FIG. 1. Optical levitation setup for measuring the polarization sensitivity of the photophoretic force. (a) The c-cut calcite crystal (CR) converts a circularly polarized single-charge vortex beam into a superposition of the radially and azimuthally polarized beam (see inset). The polarity and handedness of the vortex must be of opposite signs. The pinhole (P) selects either the azimuthal or radial polarization. The polarization state of the beam after P is varied using the system of two half-wave plates ($\lambda/2$). The lens (L) forms the trapping beam with $w_0 \sim 27 \mu\text{m}$. The cuvette (C) protects the trapped particles from air flows. The power meter (PM) measures the total power in the beam. The trapped particles are observed with a CCD camera under bright field white light (WL) illumination. (b) The intensity profile for the radial (blue line) and azimuthal (red crosses) polarizations at $z = 40 \text{ mm}$ and also shows the corresponding intensity distributions recorded after an analyzing polarizer whose transmission axis is denoted by arrow. (c) The trapping beam after L can be accurately described by Eq. (2).

As discussed in Ref. 13, the photophoretic force for a doughnut-like laser mode has both a longitudinal and transverse component. The transverse component traps the particle inside the beam laterally, whereas the longitudinal component \mathbf{F}_z in our experiments counterbalances the gravitational force $\mathbf{F}_g = -mge_z$, where m is the particle's mass, g is the free fall acceleration, and \mathbf{e}_z is the unit vector in the z -direction. Both the buoyancy force (i.e., $4\pi a^3 \rho_d/3$) and the force associated with radiation pressure (i.e., $\sim P_{\text{abs}}/c$, where c is the speed of light) are roughly two orders of magnitude smaller than \mathbf{F}_g .¹⁸ Therefore, when the particle is stabilized inside the trap, one can simply write $\mathbf{F}_z + \mathbf{F}_g = 0$.

If the spherical particles to be levitated are very large (i.e., $a \sim 50 \mu\text{m}$) compared to the wavelength of light (i.e., $\lambda = 532 \text{ nm}$), the incident beam may be thought to consist of separate rays of light which pursue their own paths.¹⁹ For a particle trapped on the axis of a cylindrically symmetric beam, the place of incidence of a ray is characterized only by its distance $r = a \sin \theta$ from the axis, where θ is the angle between the incident ray and the surface (Fig. 2). Rays hitting the surface of an absorbing particle are partially reflected and partially absorbed. We assume that the absorption occurs entirely on the illuminated surface within a thin skin layer (see caption to Fig. 3). The absorbed power P_{abs} in this case can be approximated by the difference between the power intercepted by the particle's geometrical cross section $P_{\text{in}}(z) = P(1 - \exp(-a^2/w(z)^2))(1 + a^2/w(z)^2)$ and the power contained in the reflected light. If the particle is trapped exactly at the axis of the beam (Fig. 2), the latter is given by¹⁹

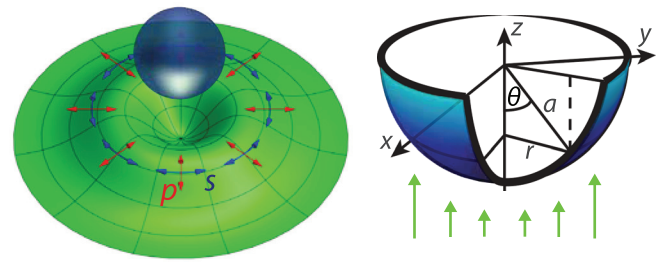


FIG. 2. The coordinate system used in the calculation of the photophoretic force for a spherical particle trapped inside a radially or azimuthally polarized laser beam given by Eq. (2).

$$P_{R(s,p)}(z) = \pi a^2 \int_0^{\pi/2} I(\theta, z) R_{s,p}^2(\theta) d \sin^2 \theta, \quad (3)$$

where $I(\theta, z)$ is described by Eq. (2) and $R_{s,p}$ stand for the Fresnel reflection coefficients for the incident light beam whose electric vector is perpendicular (s -polarized) or parallel (p -polarized) to the plane of incidence.²⁰ For a spherical particle centered in the trap, the electric field of an azimuthally polarized beam is always perpendicular to the plane of incidence (s -polarization), whereas the electric field of a radially polarized beam always lies in the plane of incidence (p -polarization). The polarization dependence of the photophoretic force for these two limiting cases becomes especially simple:

$$\mathbf{F}_{z(s,p)}(z) = 9\mu_a^2 (P_{\text{in}}(z) - P_{R(s,p)}(z)) \mathbf{e}_z / 4a\rho_a T (k_p + 2k_a). \quad (4)$$

Particles are launched into the levitation setup from the top at $z \sim 200 \text{ mm}$ with a paintbrush. At this position, the beam

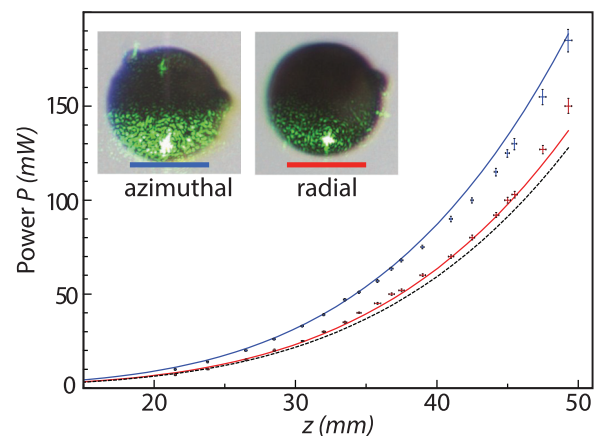


FIG. 3. Polarization-sensitive photophoresis. A hollow sphere $110 \mu\text{m}$ in diameter is trapped with the azimuthally polarized beam (strong scattering) and radially polarized beam (weak scattering) at $z = 40 \text{ mm}$. The light absorbing carbon coating is $\sim 200 \text{ nm}$ thick based on SEM-assisted measurements which were performed on several crushed spheres of similar size.⁴ Such a coating transmits less than 10% of the refracted light. The sphere's mass is estimated at 27 ng by measuring its terminal settling velocity and applying Stoke's law. The graph shows the measured (symbols) and calculated (lines) dependencies of the trapping efficiency for the sphere. The dashed line represents the situation when the sphere is considered an ideal black body, and therefore, no light is reflected from its surface. The simulations are based on $k_p = 0.17 \text{ W m}^{-1} \text{ K}^{-1}$, $\mu_a = 1.85 \times 10^{-5} \text{ N s m}^{-2}$, $\rho_a = 1.29 \text{ kg m}^{-3}$, $k_a = 0.026 \text{ W m}^{-1} \text{ K}^{-1}$, $T = 300 \text{ K}$, and the complex refractive index of the carbon coating $n' = 1.7 + 0.5i$.²¹

is wide enough for the particles to be easily placed into its dark center. By doing so, the particles are trapped laterally while falling towards the beam waist where the growing photophoretic force decelerates and finally stops them. A stable position of the particle exists at different powers. For a constant P , any changes introduced into the beam that affect the particle's stable position (i.e., the z -coordinate) indicate that the trapping efficiency of the setup has been either increased (z increases) or decreased (z decreases).

By switching from the azimuthal to radial polarization, we momentarily increase F_z by increasing P_{abs} and make the trapped particle move along the beam where the light intensity is lower. This motion will cease when the condition $F_z + F_g = 0$ is reinstated in a new stable position with a vertical position z_{rad} . Conversely, if the polarization is switched from radial to azimuthal, the particle will find a position closer to the beam waist z_{az} where the intensity is higher. If needed, the particle can be kept in the same position, provided that the laser power is adjusted accordingly in order to compensate for the introduced polarization-related changes in the trapping efficiency. By setting the angle between the fast axes of the two half-wave plates (Fig. 1(a)) somewhere between 0 and $\pi/4$, we generate a spirally polarized beam, i.e., a linear superposition of a cylindrically symmetric radial polarization and a cylindrically symmetric azimuthal polarization, and stabilize the particle in an intermediate position $z_{az} < z_{sp} < z_{rad}$.

These results are quantified in Fig. 3. We consistently observe a 20%–30% difference in the power P required to keep the trapped particle in the same position when we switch from the azimuthal to radial polarization. The effect is especially clear at low P when the destabilizing convective air flows inside the cuvette caused by the laser heating become weaker. The percentage (or relative) difference, which is solely caused by the dependence of $R_{s,p}$ on the optical constants of the trapped particle, increases with the magnitude of the real part n and the imaginary part χ of the refractive index n' of the light absorbing coating. On the other hand, the absolute difference in P depends on all the parameters in Eq. (4). Exact values of the optical and thermal parameters n' and k_p are not available in our case and are, therefore, considered fitting parameters (see captions to Fig. 3). The value of n' that we use in our analysis is typical of light-absorbing, carbonaceous substances (e.g., soot, black carbon), whereas k_p is lower than a typical value of carbon thin films and glass. This is not an unexpected result since the thermal conductivity of a thin-walled spherical shell can be assumed to be equal to that of the surrounding air.²²

The observed polarization sensitivity of photophoresis is expected to be a universal phenomenon. The photophoretic force depends on the distribution of the radiant energy absorption inside the particle,^{9,10} which, in its turn, is

affected by the polarization-dependent reflection from the particle surface. For large particles (i.e., $a \gg \lambda$), the latter is governed by the Fresnel formulae that preserve their dependence on polarization of the incident light for any material.

The polarization sensitivity of the trapping efficiency is strongly affected by the shape of the levitated objects. We have observed that the trapping efficiency of an agglomerate of the spheres can in fact be highest for any state of polarization depending on the exact configuration of the agglomerate. An analysis of photophoresis of particles with complex forms of the boundary surfaces goes beyond the scope of this paper.

In conclusion, we have observed the dependence of the photophoretic force on the light polarization and also demonstrated that a semi-quantitative theoretical analysis of this effect is possible for large and strongly absorbing spherical particles. The effect becomes very pronounced when the polarization matches the particle's geometry. For spherical particles, it is a cylindrically symmetric radial or azimuthal polarization. This implies that by tuning the polarization state one can selectively affect the photophoretic force acting on different types of particles.

¹A. Ashkin, *Phys. Rev. Lett.* **24**, 156–159 (1970).

²M. Lewittes, S. Arnold, and G. Oster, *Appl. Phys. Lett.* **40**, 455 (1982).

³Yu. I. Yalovoy, V. B. Kutukov, and E. R. Shchukin, *J. Colloid Interface Sci.* **57**, 564 (1976).

⁴V. G. Shvedov, A. V. Rode, Y. V. Izdebskaya, A. S. Desyatnikov, W. Krolikowski, and Yu. S. Kivshar, *Phys. Rev. Lett.* **105**, 118103 (2010).

⁵V. G. Shvedov, A. V. Rode, Y. Izdebskaya, A. Desyatnikov, W. Krolikowski, and Yu. S. Kivshar, *Opt. Express* **18**, 3137 (2010).

⁶P. Zhang, Z. Zhang, J. Prakash, S. Huang, D. Hernandez, M. Salazar, D. N. Christodoulides, and Z. Chen, *Opt. Lett.* **36**, 1491 (2011).

⁷V. G. Shvedov, C. Hnatovsky, A. V. Rode, and W. Krolikowski, *Opt. Express* **19**, 17350 (2011).

⁸C. Alpmann, M. Esseling, P. Rose, and C. Denz, *Appl. Phys. Lett.* **100**, 111101 (2012).

⁹S. Arnold and M. Lewittes, *J. Appl. Phys.* **53**, 5314 (1982).

¹⁰W. M. Greene, R. E. Spjut, E. Bar-Ziv, J. P. Longwell, and A. F. Sarofim, *Langmuir* **1**, 361 (1985).

¹¹M. Pope, S. Arnold, and L. Rozenshtein, *Chem. Phys. Lett.* **62**, 589 (1979).

¹²S. Arnold and Y. Amani, *Opt. Lett.* **5**, 242 (1980).

¹³A. S. Desyatnikov, V. Shvedov, A. Rode, W. Krolikowski, and Yu. S. Kivshar, *Opt. Express* **17**, 8201 (2009).

¹⁴N. O. Eckerskom, N. Zeng, V. G. Shvedov, W. Krolikowski, and A. V. Rode, *Journ. Opt.* **14**, 055302 (2012).

¹⁵L. D. Reed, *J. Aerosol Sci.* **8**, 123 (1977).

¹⁶C. Hnatovsky, V. Shvedov, W. Krolikowski, and A. Rode, *Phys. Rev. Lett.* **106**, 123901 (2011).

¹⁷Q. Zhan and J. R. Leger, *Opt. Express* **10**, 324 (2002). PMID:19436363, <http://www.opticsexpress.org/abstract.cfm?oe-10.7-324>.

¹⁸In our experiments P_{abs} is ~ 1 mW and the corresponding photon pressure force is $\sim 3 \times 10^{-12}$ N. The particle volume density is ~ 40 kg/m³, i.e., more than 30 times larger than ρ_a . F_g for a 30-ng particle is $\sim 3 \times 10^{-10}$ N.

¹⁹H. C. van de Hulst, *Light Scattering by Small Particles* (Dover, New York, 1981).

²⁰M. Born and E. Wolf, *Principles of Optics*. (Pergamon, Oxford, 1993).

²¹T. C. Bond and R. W. Bergstrom, *Aerosol Sci. Technol.* **39**, 1 (2005).

²²A. J. Bullen, K. E. O'Hara, D. G. Cahill, O. Monteiro, and A. von Keudell, *J. Appl. Phys.* **88**, 6317 (2000).